

Imaging the Reactivity and Width of Graphene's Boundary Region

Huda S. AlSalem,^{a,b,c} Soha T. Al-Goul,^{d,e} Alejandro García-Miranda Ferrari,^{f,g} Dale A. C. Brownson,^{f,g} Luis Velarde,^d Sven P. K. Koehler^{f}*

^a School of Chemistry, The University of Manchester, Oxford Road, Manchester, M13 9PL, United Kingdom.

^b Photon Science Institute, The University of Manchester, Oxford Road, Manchester, M13 9PL, United Kingdom.

^c School of Chemistry, Princess Nourah bint Abdulrahman University, Riyadh, Saudi Arabia.

^d Department of Chemistry, University at Buffalo, State University of New York, Buffalo, New York 14260-3000, United States.

^e School of Chemistry, King Abdulaziz University, Rabigh, Saudi Arabia.

^f Department of Natural Sciences, Manchester Metropolitan University, Chester Street, Manchester, M1 5GD, United Kingdom.

^g Manchester Fuel Cell Innovation Centre, Manchester Metropolitan University, Manchester M1 5GD, United Kingdom.

Experimental setup:

The broadband SFG spectrometer¹ is shown in Figure S1 and consists of a regenerative amplifier (Legend HE+, Coherent, Inc.) seeded by a titanium-sapphire oscillator (Vitara, Coherent, Inc.). The amplifier outputs ~804 nm with a pulse width of ~35 fs and a 1 kHz repetition rate. The output is split by a beam splitter to generate mid-infrared (IR) pulses using an optical parametric amplifier (OPA) with difference frequency generation (DFG) of the signal and idler pulses, while another portion is used to generate 400 nm narrowband picosecond pulses (~5 ps) in a second harmonic bandwidth compressor (Light Conversion) that pumps a ps OPA to

generate tunable narrowband ($\sim 7 \text{ cm}^{-1}$) visible (Vis) pulses. The broadband ($\sim 400 \text{ cm}^{-1}$) IR frequency was centred at 3150 cm^{-1} and the up-converting visible wavelength was set to 660 nm . The angle of incidence with respect to the surface normal for the IR and Vis beams were 70° and 45° , respectively. The polarisation of all beams was kept at *ppp* (SFG/Vis/IR). A raw spectrum of phenyl-functionalised graphene on gold is shown in Figure S2. Each spectrum was acquired for 1 min, background subtracted, and normalised to the non-resonant SFG response of a bare gold film to yield spectra such as those shown in Figure 1 in the main text. The Raman maps were recorded using a HORIBA LABRAM HR EVO instrument equipped with a Marzhauser translation stage. The maps were recorded using $<1 \text{ mW}$ of a 488 nm excitation laser, 600 gr/mm grating and $50\times$ objective lens.

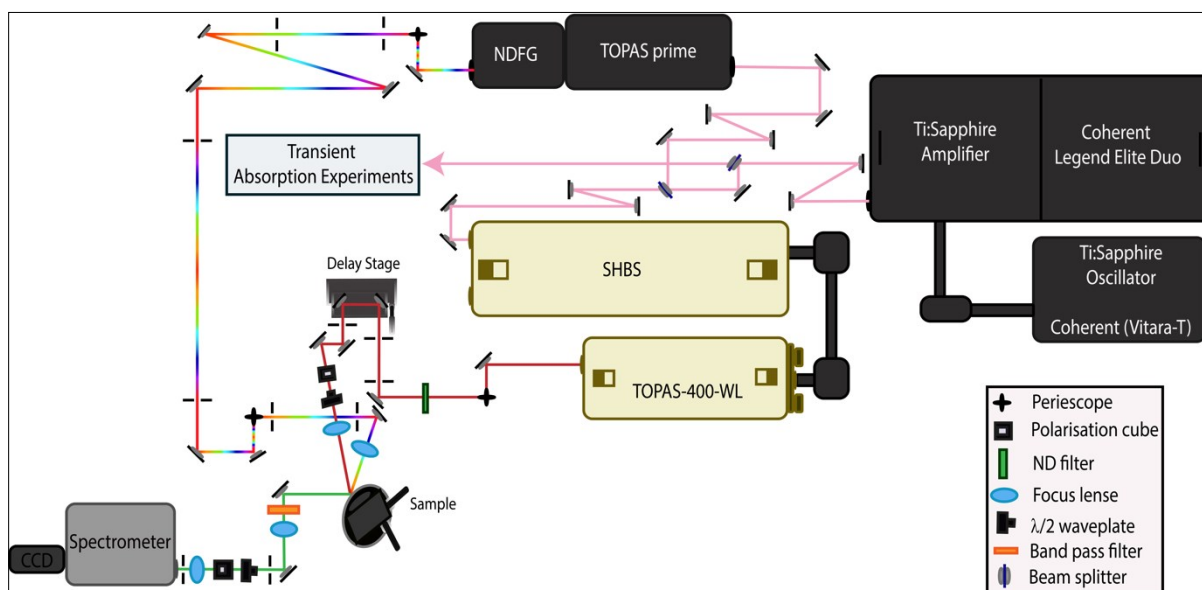


Figure S1: Schematic diagram of the SFG spectrometer.

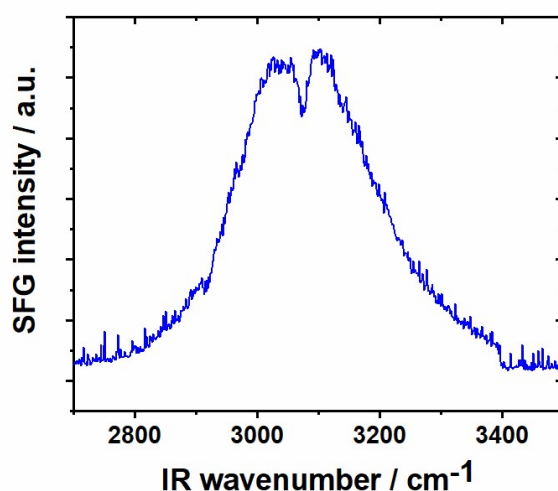


Figure S2: Raw SFG spectrum of phenyl-functionalised graphene on gold after 1 min. acquisition time. The polarisation was kept at *ppp* (SFG/Vis/IR).

Discussion of Raman spectra and maps:

The peak positions averaged over all pixels of the Raman maps (Fig. 1 e and f) which indicate the presence of graphene before functionalisation are 1585 cm^{-1} and 2711 cm^{-1} for the G peak and the 2D peak, respectively, with a D peak appearing at 1391 cm^{-1} after functionalisation. It is known that plasmons can be generated in gold surfaces, red-shifting the peak positions by as much as 10 cm^{-1} for the G peak;^{2,3} however, these effects are small at gold thicknesses of $\sim 50\text{ nm}$ as used in our sample preparation. Surface plasmons also cause an increased intensity of all bands, but in particular the G band, which we observe in our Raman spectra, as well as a slight broadening of the bands. Our G peak position of 1585 cm^{-1} also indicates almost undoped graphene before functionalisation.³

For a spatially higher-resolved analysis of the Raman data, we performed a correlation analysis of the G and 2D peak positions for all pixels in the Raman maps

(resolution $0.5\ \mu\text{m}$, but recorded at step sizes of $50\ \mu\text{m}$ due to the large initial area of $0.4 \times 2.35\ \text{mm}^2$ imaged) for which graphene peaks were recorded, roughly half the size of the original sample, i.e. $0.4 \times 1.1\ \text{mm}^2$ (left half of Fig. 1 e and f), shown in Fig. S3. A shift in peak positions can be observed in a) and b) for the two pixel columns furthest right, i.e. around 0 where the graphene boundary is located. While the resolution of the data does not allow a more quantitative analysis, the correlation plot in Fig. S3 c), esp. for pristine graphene near the edge (blue circles), shows a shallow positive slope which may be indicative of strain, while the far steeper, almost vertical alignment of data points after functionalisation might indicate doping. It is worth noting, however, that the maps in a) and b) show a fairly homogenous Raman peak position behaviour for the largest part of the area imaged and only start changing $\sim 100\ \mu\text{m}$ away from the edge, while the vSFG data indicates that functionalisation also takes place further away from the boundary region, even when taking into account the inferior spatial resolution in the vSFG experiments.

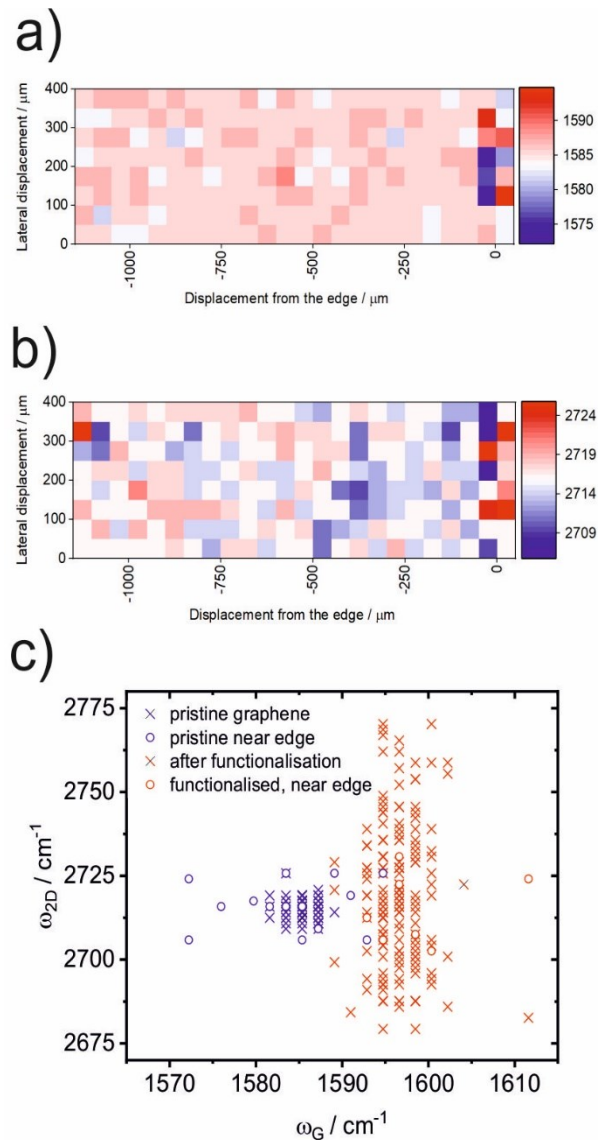


Figure S3: Peak positions of the a) G band and b) 2D band before functionalisation for the area of the sample containing graphene, i.e. left half of Fig. 1 e) and f), where 0 along the x axis is the position of the edge. c) Correlation plot of the Raman maps before (blue) and after (red) functionalisation, where circles are data points from the two pixel columns furthest right in a) and b), i.e. around the graphene boundary.

Sample preparation:

The graphene samples were first grown on copper foil and subsequently transferred onto a gold substrate using a modified version of the polymer-free CVD graphene transfer method adapted from Zhang *et al.*;⁴ this polymer-free transfer method uses ammonium persulfate as an etching solution to remove the copper. The graphene sheets are then transferred onto a deionised water/hexane interface to clean away

any etching products that might have remained in solution. Finally, the free-floating graphene sheet is transferred onto a gold substrate with one edge of the graphene sheet exposed (i.e. the edge is roughly in the middle of the substrate) in order to study the reactivity of the boundary region of graphene.

The graphene sheets were phenyl functionalised using benzene diazonium tetrafluoroborate salt following the method by Strano *et al.*,⁵ see Figure S4 a). The diazonium salt was synthesised from aniline and sodium nitrite in the presence of tetrafluoroborate acid as reported by Lackner and Fürstner.⁶ A SFG spectrum of the gold substrate functionalised with the diazonium salt is shown in Figure S4 b), where the raw data is fitted to equation

$$I = A_0 e^{i\phi} + \left| \sum_{i=1}^n \frac{A_n}{\omega_n - \omega_{IR} - i\Gamma_n} \right|^2 \quad \text{Eqn. S1}$$

where A_0 is the non-resonant contribution while $e^{i\phi}$ accounts for the phase difference between the resonant and non-resonant signal with A_n , ω_{IR} and ω_n representing the amplitude, centre wavenumber, and linewidth of the n^{th} vibrational mode, respectively.

This spectrum provides a possible explanation as to why the SFG signal does *not* decay to zero as one scans the laser beams over the boundary region into an area not initially covered by graphene, see Figure 2 c) in the main text.

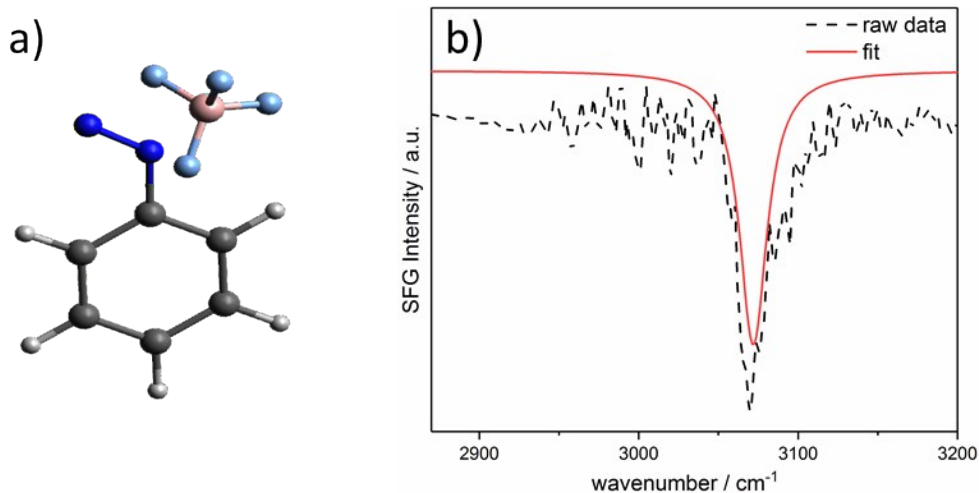


Figure S4: a) Structure of the benzene diazonium tetrafluoroborate salt and b) SFG spectrum of the gold substrate (without any graphene present) functionalised with the diazonium salt.

Discussion of Laser Polarisation and Orientation:

The vSFG intensity is related to the orientation of the molecular vibration that is probed with respect to the polarisation of the laser beams involved, and proportional to the square of the number density of surface functional groups. The polarisation in our experiments is *ppp* (SFG/Vis/IR) and remains unchanged throughout the experiments. For spectra recorded in the *ppp* polarization combination, both the *xxz* and *zzz* components of the resonant second-order susceptibility must be considered (*z*-axis along the surface normal).⁷ It has been shown that the effective second-order nonlinear susceptibility for *ppp* on metal and carbon substrates is dominated by the *zzz* component.⁸ Since we have previously established that the phenyl groups chemisorbed to graphene terraces are on average aligned along the surface normal, and since any possible deviation from this perpendicular alignment at the graphene edges would hence *reduce* the vSFG intensity, we conclude that molecular orientation alone cannot account for the significant intensity change in the boundary region.

References:

- 1 S. T. Algoul, S. Sengupta, T. T. Bui and L. Velarde, *Langmuir*, 2018, **34**, 9279–9288.
- 2 B. G. Ghamsari, A. Olivieri, F. Variola and P. Berini, *Phys. Rev. B - Condens. Matter Mater. Phys.*, 2015, **91**, 201408.
- 3 M. Kalbac, V. Vales and J. Vejpravova, *RSC Adv.*, 2014, **4**, 60929–60935.
- 4 G. Zhang, A. G. Güell, P. M. Kirkman, R. A. Lazenby, T. S. Miller and P. R. Unwin, *ACS Appl. Mater. Interfaces*, 2016, **8**, 8008–8016.
- 5 Q. H. Wang, Z. Jin, K. K. Kim, A. J. Hilmer, G. L. C. Paulus, C. J. Shih, M. H. Ham, J. D. Sanchez-Yamagishi, K. Watanabe, T. Taniguchi, J. Kong, P. Jarillo-Herrero and M. S. Strano, *Nat. Chem.*, 2012, **4**, 724–732.
- 6 A. D. Lackner and A. Fürstner, *Angew. Chem. Int. Ed. Engl.*, 2015, **54**, 12814–12818.
- 7 P. J. N. Kett, M. T. L. Casford and P. B. Davies, *J. Phys. Chem. Lett.*, 2012, **3**, 3276–3280.
- 8 J. L. Achtyl, A. M. Buchbinder and F. M. Geiger, *J. Phys. Chem. Lett.*, 2012, **3**, 280–282.